

A Review on Friction Stir Processing of Magnesium Alloys

¹omkar Ankush Chavan

²tushar Kishor Chavan

³shashikiran Bharat Taur

⁴shubham Rajuvaral

⁵h. A.Deore

¹²³⁴UG Students and ⁵Assistant Professor at Department of Mechanical Engineering, Smt. Kashibai Navale College Of Engineering, Vadgaon(BK), Savitribai Phule Pune University(SPPU)

Abstract

Friction Stir Processing (FSP) works on principle of Friction Stir Welding. Through intense localized plastic deformation FSP changes properties of materials. Surface properties, such as wear resistance, hardness and strength can determine the service life of components in many industrial applications. The paper reviewed different factors affecting magnesium alloys during FSP. Magnesium alloys are used in variety of different applications. They are used when looking for weight reduction without compromising overall strength. Magnesium alloys are also used in automotive, aerospace applications. In this process we can make different solid state process composition in which single phase as well as multi-phase composition can be formed. In two phase surface composition different additives like SiC, CNT, B₄C, etc can be used. In this review article we studied that FSP can be done by considering factors like tool material, rotational speed, processing speed. FSP modifies microstructure of single component or multiple workpieces.

Keywords: Friction Stir Processing, Magnesium alloy, Microstructure, Grain Size, Mechanical property.

1. Introduction: FSP has such conceivable to give mass scale production with fine grain structure and improved mechanical properties[1]. During FSP, properties can also be improved by variation of heating input on plate[2,3]. In FSP, the tool rotational speed results in stirring and mixing of the material around the rotating pin which in turn increases the temperature of the metal[4]. Well labelled diagram of the FSP method is shown in Figure 1. This process includes heating and plastic deformation of the material by friction created by a tool, rotating and transverse movement along the surface of the base plate. The heating and plastic deformation of the material is to be done using a rotating tool, which penetrates the material along the surface of material. When the tool is in rotation and the material continuously heated by friction and plasticized near the tool, the entire system moves along the line. The plasticized and heated material is forced towards the rear end, where it is mixed and compacted by deformation before being cooled down. The movement of the tool set at the correct angle results in heating, intensive mixing, and compaction of the deformed material[5].

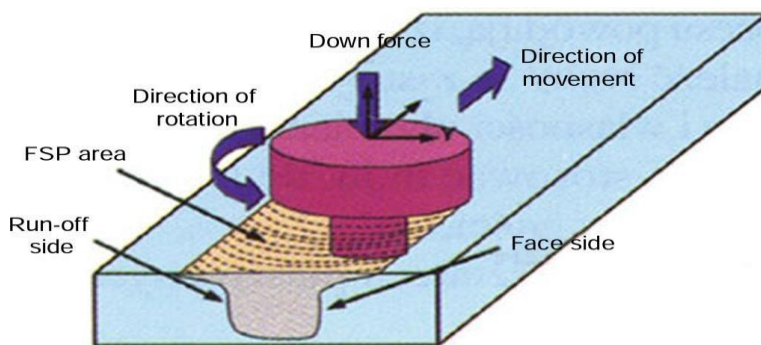


Fig.1. Method of modification of surface layers by friction with mixing of material – FSP process diagram[5].

Materials like aluminium, titanium, magnesium used in wide range of applications of the field of aerospace and automotive parts because of its lightweight. Pure magnesium is one of the lightest

structural metals with a density of 1.74 g/cm^3 , while aluminium is 2.70 g/cm^3 and steel 7.85 g/cm^3 among this lightweight material magnesium is preferred one because of its high strength to weight ratio. Magnesium alloys has wide range of application in aerospace, automotive and electronic industries because of its properties of light weight, high specific stiffness, high specific strength, and so on[6]. A mass reduction of 20% can be achieved by replacing aluminium with a AZ31 Mg wrought sheet, with similar stiffness and strength requirements in large surfaced/thin-walled applications, and even 50% of reduction if replaced by steel[7]. AZ31 magnesium alloy is commercially available in sheet form, and has good mechanical properties. But the alloy have very limited ductility and brittle- like behaviour at room temperature. Recent results however indicated that it is possible to form AZ31 sheets at elevated temperatures under certain conditions, and even achieve superplastic-like behaviour. The results suggested improved ductility and formability can be achieved by refining the grain structure of the sheet. FSP is the effective method for microstructural modification of sheet metals[8].

2. Friction stir processingparameters

The major parameters affecting FSP are - (1) Tool geometry, (2) Tool material, (3) Machine parameters, (4) Additives.

2.1 Toolgeometry:-

Tool geometry is the most important aspect of FSP process. The tool geometry plays a vital role in material flow and hence governs the traverse rate at which FSP can be conducted. An FSP tool consists of a shoulder and a pin as shown schematically in Fig. 2. The tool has two main functions: (a) material flow, (b) localized heating. In the starting stage of tool plunge, the heating results in friction between pin and workpiece and also due to the deformation of material. The tool is inserted until the shoulder comes in contact with the workpiece. Major part of heating due to friction between the shoulder and workpiece. From the heating concern, the relative size of shoulder and pin is important and the other design features are not critical. The shoulder also provides impedance for the heated volume of material. The another function of the tool is to ‘stir’ and ‘move’ the material. The homogeneity of microstructure and properties are regulated by the tooldesign[9]

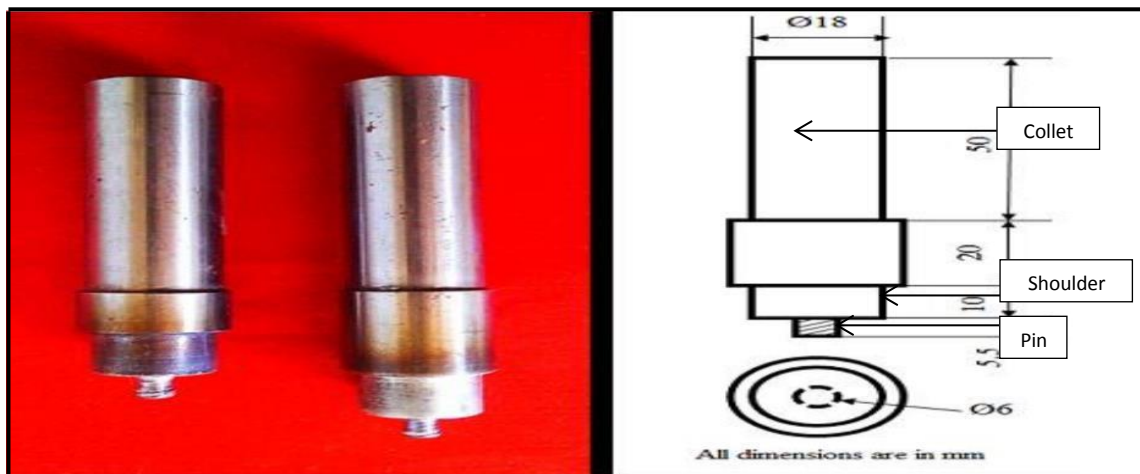


Fig.2.Fabricated FSP Tool [10].

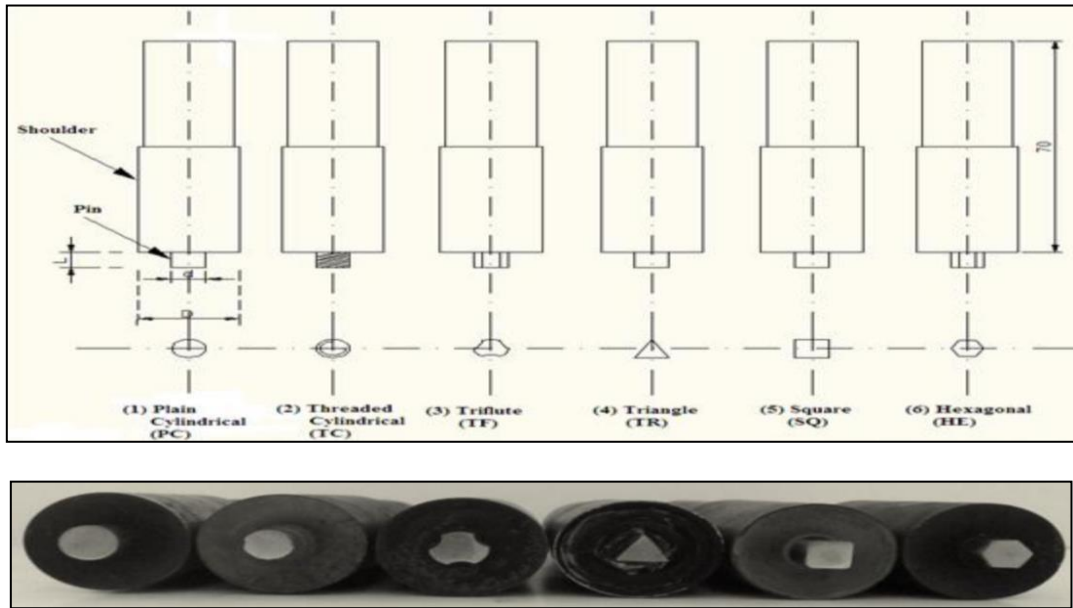


Fig. 3 Straight flat-bottom FSP tool pin profiles with its geometry [11].

2.2 Toolmaterial:-

From the analysis carried out it has been proved that SS tool material provided fine grained microstructures and better mechanical properties as compared to HSS. As shown in table 1 gives wide idea that use of SS material gives better characteristic than HSS.

Rotational speed(rpm)	Tool materials	Ultimate tensile strength(Mpa)	Yield strength(Mpa)	Elongation (%)	Hardness(HV)
900	SS	96.18	71.52	1.39	70
	HSS	129.77	94.51	2.48	66
1120	SS	181.94	139.5	4.02	75
	HSS	135.15	100.71	3.32	70
1400	SS	171.12	129.86	2.91	69
	HSS	186.76	139.1	5.00	71
1800	SS	155.04	117.69	2.24	70
	HSS	152.55	113.46	4.08	68
Base Metal		215	171	14.7	69

Table I. Effect of Rotational speed and tool material on mechanical properties of AZ31B Mg alloy using SS tool and HSS tool[12].

The low rotational speeds provided high stirred zone micro hardness values with respect to the base material. For specific tool material and tool rotational range high strength properties can be achieved in the stir zone. A tool rotational speed of 900 rpm have shown lower yield strength, ultimate tensile strength, percentage of elongation, weld nugget hardness and impact test compared to a tool rotational speed of 1120 rpm. A rotational speed of 1400 rpm as well as 1800 rpm has shown tensile strength properties lower than a rotational speed of 1120 rpm [13].

2.3 MachineParameters:-

Major machine parameters influencing the FSP are – Rotational speed, Traverse speed.

Rotational speed (rpm)	Traverse speed (mm/min)	Tilt angle (Degree)	Tensile Strength (N/mm ²)	Micro hardness (HV)
900	24	0	190	78
	32	1	237	83
	40	2	222	81
1150	24	1	239	85
	32	2	242	83.6
	40	0	226	87
1400	24	2	181	76.1
	32	0	196	83
	40	1	179	81
Parent material			215	79.0

Table II. Effect of Rotational speed and Traverse speed on mechanical properties of AZ31B[14].

2.3.1 Effect of tool rotational speed

At lower rotational speed (900 rpm), the mechanical properties are lower, because of insufficient heat generation results in poor plasticisation zone and insufficient deformation by poor stirring action as well as due to the tool pin are the reasons to decrease in mechanical properties. Mechanical properties of material are improved by providing sufficient heat to plasticise the material in order to get complete deformation with proper grain refinement and material flow through dynamic recrystallization with higher rotational speeds. As shown in Table II, at rotational speed of 1150 rpm, tensile strength and hardness are improved. As the rotational speed (1400 rpm) further increases results in higher temperatures in the stirred zone than the optimal, leads to the grain growth that decreases the tensile strength and hardness. Hence, optimal rotational speed must be preferred to avoid incomplete deformation. Hence, at rotational speed of 1150 rpm the best mechanical properties were obtained[15].

2.3.2 Effect of traverse speed

Mechanical properties of processed material are also affected by Traverse speed. As shown in Table II, a lower traverse speed (24 mm/min) causes slower cooling rate which provides sufficient time for grain growth results in lower hardness and tensile strength. To limit the amount of grain growth, the time of the exposure of processed area to frictional heat generated from the rotating tool is controlled. In order to obtain better mechanical properties, optimum values of traverse speed are preferred. As per analysis at traverse speed of 32 mm/min are preferred for obtaining best mechanical properties for all the rotational speeds[16].

2.4 Effect of additives

By using additives like SiC, CNT mechanical strength of Mg alloy can be improved.. 4, 8 and 16 % (v/v) composition of SiC particles or carbon nanotubes (CNT) was added to AZ31 alloy. With FSP microstructure, micro-hardness and tensile strength of the composites were observed. Addition of additives decreased the size of the grains and increased structural uniformity and micro-hardness. Micro-hardness is increased from 67 HV to 112 HV for 8% SiC and to 108 for 8% CNT [17].

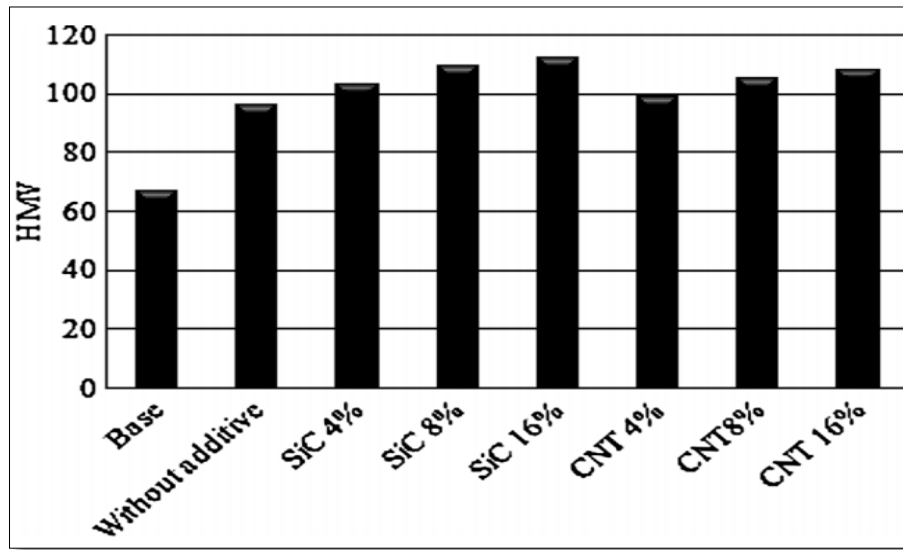


Fig. 3. Average values of micro hardness in the raw material, four times FSP process without reinforcing particle and composites contains 4, 8 and 16 percentages of SiC nanoparticles and carbon nanotubes[18]

Results for yield, ultimate stress, and ductility are listed in Table III. FSP without additives resulted in an increase in ultimate stress and ductility and decrease in yield stress [19]. Due to increasing percentage of SiC particles there is increase in yield stress and decrease in elongation[20].

	Yield stress (Mpa)	Ultimate stress (Mpa)	Elongation (%)
Base material	110.14	251.80	22.82
Without additives-1 pass	56.71	267.35	33.01
Without additives-4 pass	57.3	290.70	40.63
SiC-4%	75.42	292.21	34.84
SiC-8%	105.17	283.83	17.80
SiC-16%	122.27	244.13	12.89
CNT-4%	77.11	253.25	26.14
CNT-8%	107.73	230.73	13.92
CNT-16%	132.38	222.72	8.30

Table III. The values of yield stress, ultimate stress and ductility[21].

3. Microstructural Modification

3.1 Effect of rotational speed on microstructure:

The FSP tool was rotated in clockwise direction with different rotational speed 1300, 1500, 1700 rpm with traverse speed at 50 mm/min and tilt angle at 2.5°. For optical examination, the samples were sectioned, cold mounted, polished by silicon dioxide paste with grain size of 1 μm and finally etched in a solution of oxalic acid(2g), nitric acid (1mL) and pure water (98mL), and then observed under ZEISS optical microscope[22]. Figure 4 shows the cross-sectional macrostructure of the FSPed sample with a rotating speed of 1500 rpm. Three distinct regions are present in the final macrostructure: heat affected zone (HAZ), thermo-mechanically affected zone (TMAZ) and stir zone (SZ)[23]. Compared with the advancing side (AS) and retreating side (RS), has a much sharper and clearer boundary which can be visible. The microstructure of AZ31 magnesium alloy consisted of elongated, uneven distributed grains along the rolling directions (as shown in figure 2 (a)). After FSP the equiaxed grains were found in the SZ. FSPed samples found significantly refined grains as compared with the AZ31 base alloy. At a constant traverse speed, the average grain size was respectively 11.82 μm, 12.93 μm and 14.50 μm (as shown in figure 2 (b),(c),(d)), getting larger with the increasing of rotating speed[24].



Fig.4 Electronic cross-sectional macro-image of FSPed sample with a rotating speed of 1500 rpm[25].

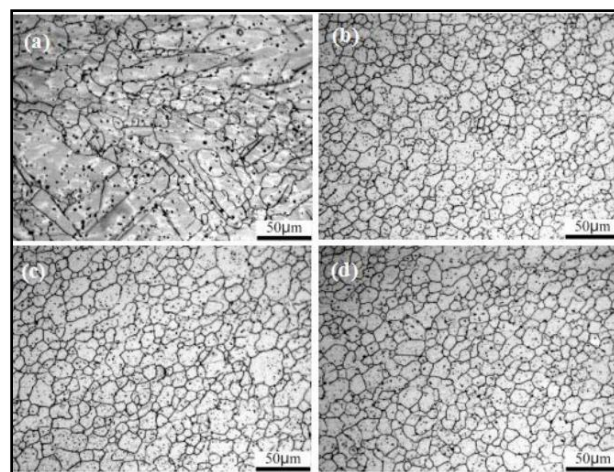


Fig.5 Microstructure of AZ31 base alloy and SZ of FSPed samples. (a) AZ31 base alloy (b) 1300rpm
(c) 1500rpm (d) 1700rpm[26]

3.2 Effect of additives on microstructure:

Figure 6 shows images from the optical microscope. The figure shows the microstructure of the base material (Fig. 6a), specimens without reinforcement (Fig. 6b), 4 % nanotubes (Fig. 6c) and 4 % SiC nanoparticles (Fig. 6 d). The base material shows a non-uniform structure with 18 μm grains. The average grain size of the AZ31 structure after four FSP passes and cooling was 6.4 μm without reinforcing materials, 3.08 μm with 4 % CNTs, 2.04 μm with 4 % SiC. Figure 6 shows that the SiC

nanoparticles and CNTs decreased the size of the grains in the structure and made the structure more uniform. Decreasing the linear speed of the FSP increased the size of the grains in materials with no reinforcing phase and in materials containing reinforcing particles in response to the extreme increase in specimen temperature. The reinforcing particles prevented a marked increase in the size of the grains, even at high temperatures. Hence 4% SiC gives more refined grain as compared to microstructure with 4% CNT[27].

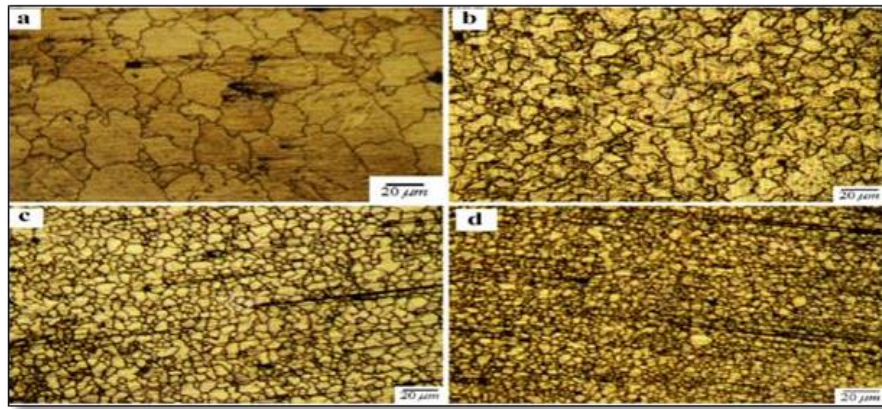


Fig. 6 The material texture in a) the base material, b) after four passes of FSP without reinforcing particles, c) with 4 % CNT, d) with 4 % SiC [28].

cooling during FSP prevented the excessive growth of grains. The distribution of 4, 8 and 16 % (v/v) SiC particles in the AZ31 alloy can be seen in Fig. 7a)–c). As shown, as the percentage of SiC particles increased, they were increasingly scattered among the magnesium grains and were uniformly distributed. Similar results were reported elsewhere [29, 30, 31]. A uniform distribution of CNTs in the AZ31 alloy was not observed using SEM; Izadi and Gerlich [32] reported similar results for aluminium 5059. In their study, damage and deformation to nanotubes increased as the number of passes increased and, in some areas, agglomeration of nanotubes were observed.

EDS analysis detected a high percentage of carbon in the areas of interest, indicating a concentration of nanotubes. Figure 4a shows the average concentrations for three samples each at percentages of 4, 8 and 16 % (v/v) CNTs. The CNTs were relatively long and they easily entangled, which might have resulted in their undesirable distribution in the AZ31 alloy. Lim et al. [33] also observed that, after FSP, CNTs were entangled and not uniformly distributed throughout the aluminiummatrix.

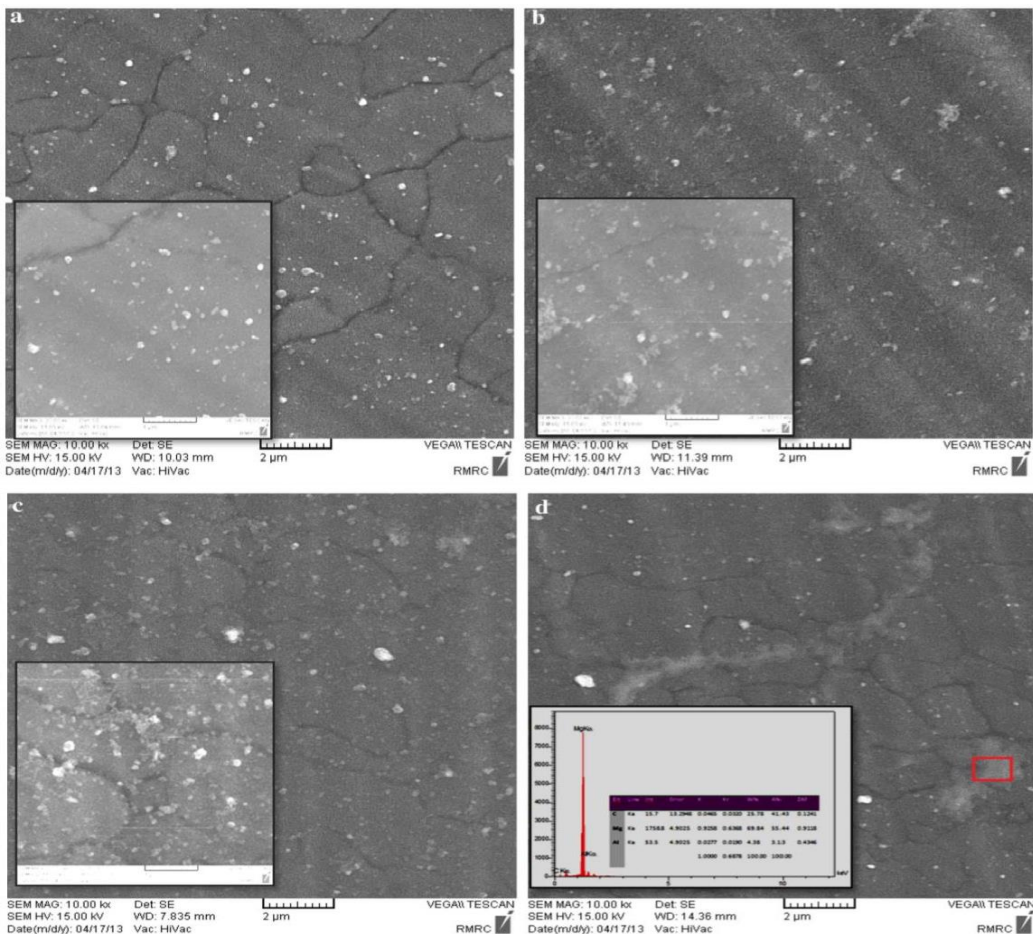


Fig. 7 a) Distribution of 4 % SiC nanoparticles, b) 8 % SiC nanoparticles, c) 16 % SiC nanoparticle, d) carbon nanotubes agglomeration within the AZ31 alloy[34].

3.3 Effect of processing speed on microstructure:

The average grain size of the base material was $16.5 \mu\text{m}$ and its optical microstructure is as shown in Fig.7 (a). After FSP process it is observed from the microstructures that the grains were refined and the microstructure were homogeneous having finer grain size than the base metal, because of refinement process during processing due to severe plastic deformation of the material. As compared to base material the sample processed with a 24mm/min traverse speed exhibited homogenous grain structure smaller grains because of excessive heat generation during processing, which results in grain growth of the material after refinement. Also at 32mm/min traverse speed more homogeneous equiaxed grains of average size of $6.2 \mu\text{m}$ were found in the samples. Optimal heat input results in intense plastic deformation[35].

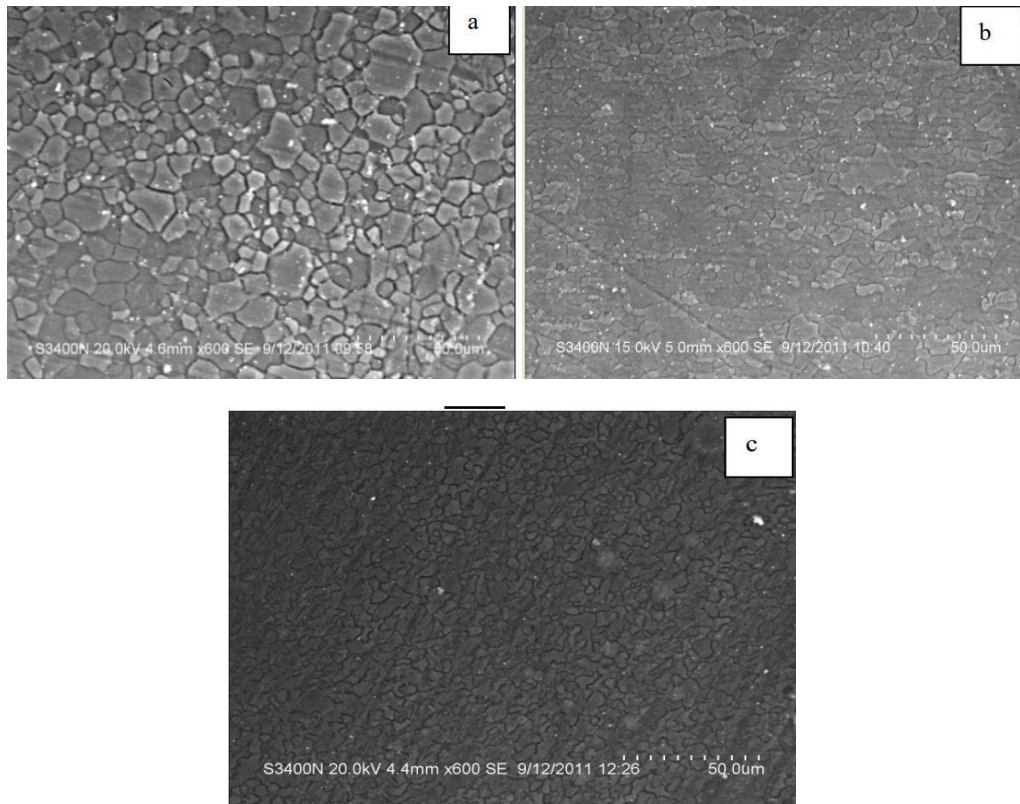


Fig. 7 (a) Optical microstructure base material (b) FSPed material at traverse speed of 24mm/min (c) 32mm/min [36].

4. MechanicalProperties:

4.1 Effect of FSP on tensilestrength

Tensile strength and elongation values of the samples studied are given in Table IV. It can be seen from Table IV that for all FSPed samples, the strength and ductility values are higher than those for as-received sample. The tensile test results indicates that for the FS-processed sample with no particle addition both strength and ductility values are higher than those for one-pass processed sample. This can be assigned to agglomeration and nonhomogeneous distribution of particles during one-pass processing which accelerate nucleation and growth of cracks during tensile test [37].

Sample	UTS (Mpa)	Elongation (%)
Base material	124.56	10.1
FSP-No additives	203.65	14.04
FSP-SiC		
One-pass	171.57	12
Two-pass	306.63	13.05
Four-pass	390.71	16.56

Table IV. Comparison of mechanical properties relating to FS-processed samples and as-received sample [38].

As can be seen in Table I, the increase of pass number during FSP results in more grain refinement and more homogeneous distribution of reinforcing particles which delay crack initiation and growth. There is uncertainty in increment of strength and ductility as pass number enhances. Because of the breakup of coarse dendrites, elimination of porosity, and refinement of matrix grains there is an increase in mechanical properties, this has also been observed by other researchers [39,40].

4.2 Effect of FSP on micro-hardness

The micro-hardness increased as a result of three factors after the addition of reinforcing particles using FSP: fine grain size, the percentage of reinforcing phases in the matrix, and quench hardening from the thermal expansion coefficient of the reinforcing particles and the matrix [41]. The micro-hardness of different samples is illustrated in Fig. 3. As seen, the micro-hardness increased from 67 Vickers for the base material to 108 Vickers for the composite with 16 % CNT and 112 Vickers for the composite with 16 % SiC. This can be represented as:

$$H_{\text{composite}} = H_{\text{matrix}} V_{\text{matrix}} + H_{\text{particle}} V_{\text{particle}}$$

Where H is the micro-hardness and V is the volume (v/v). Fig. 3 shows that the micro-hardness of the composite increased as the percentage of reinforcing phase increased [42]. This suggested that AZ31 alloy containing SiC nanoparticles displayed greater micro-hardness than AZ31 alloy containing CNTs. An evaluation of the microstructure shows that a more uniform distribution of SiC nanoparticles in the matrix created a structure with a finer grain size that increased the micro-hardness of the composites. An increase in micro-hardness resulting from the uniform distribution of SiC nanoparticles was previously reported [43, 44].

4.3 Effect of FSP on wear

As per Sarkar [45], abrasive wear occurs due to hard particles embedded in either hard, rough surface or a soft surface slides over a softer material. Hence ploughing action takes place, and scratches or parallel furrows in the direction of motion form. As shown Fig. 8, In processed samples grooves are not as deep as that in base metal. This relates to the low hardness of base material as compared to processed samples. High hardness resists the formation of deep grooves during wear.

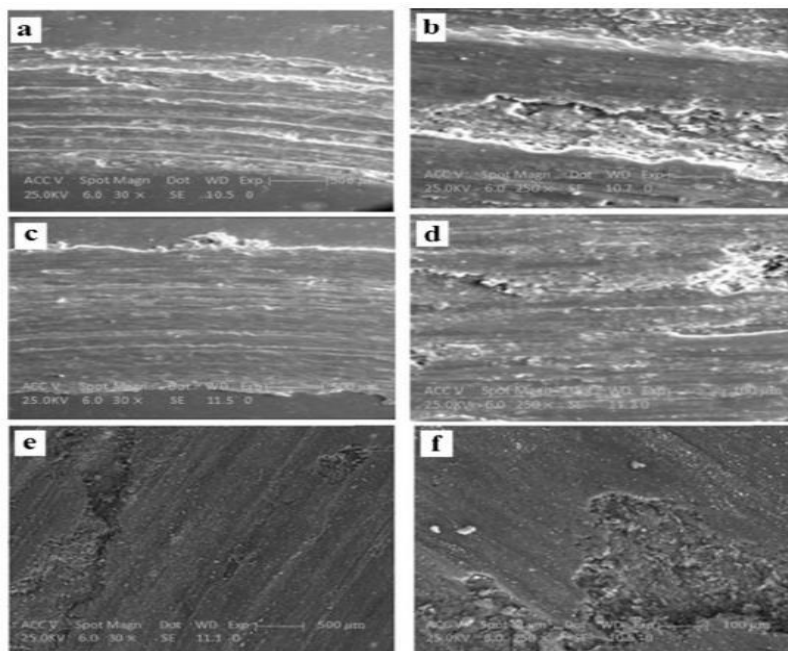


Fig. 8 Worn surfaces of base material (a, b) and FS-processed samples (c–f) after wear test (c, d relate to samples FS-processed with SiC particles while e, f relate to samples processed with Al_2O_3 particles)[46]

Fig. 9 shows wear rate of different samples . Figure shows wear rate of base metal is greater than other samples, and As pass number increases wear rate decreases. As per Archad relation [47], when wear rate decreases then hardness increases. Also, it comes from Fig. 8 that wear rate of processed samples using Al_2O_3 , SiC particles have nearly the same wear resistance [48].

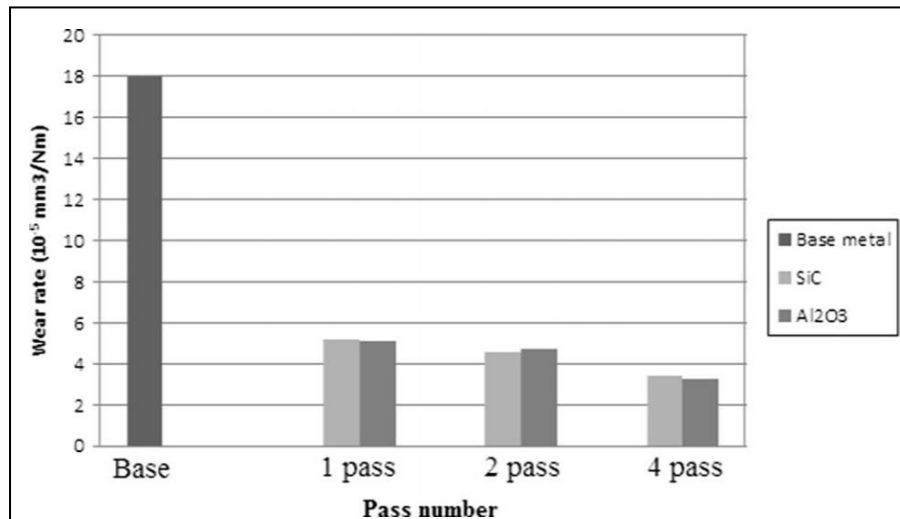


Fig. 9 Wear rate of FS-processed samples and base material[49].

5. Conclusion:

In this review article friction stir processing is briefly explained. We studied different parameters like tool geometry, tool material, machine parameters, additives and their effect on microstructure and mechanical properties are as follows-

- 1) As per Mishra R S ,they concluded that SS tool material provided fine grain microstructure and better mechanical properties as compared to HSS toolmaterial.
- 2) From research performed by GantaVenkateswarlu, M Joseph Davidson , Pulla Sammaiah.,at lower rotational speed (900 rpm), mechanical properties are lower. But as we go up to the speed of 1150rpm, mechanical properties were improved. Beyond 1150rpm due to temperature increase leads to grain growth that decreases mechanical properties. Hence the optimum range is to be preferred in between 800 rpm to 1150 rpm. Finer grain size is obtained in thisrange.
- 3) As per research of Ganta Venkateswarlu , M Joseph Davidson , Pulla Sammaiah., when there is increase in traverse speed from 24 mm/min to 32 mm/min, mechanical properties are improved as well as grain structure becomesfiner.
- 4) As per reaserch done by A.Alavi Nia, S.H.Nourbakhsh ,the different additives like SiC , CNT etc. are used with magnesium alloy for carrying out FSP, results concluded that processed sample using SiC showed better mechanical properties as compared sample using CNT.

6. References:

1. Blawert C, Hort N, and Kainer K U, Trans Indian Inst Met 57(4) (2004)397.
2. A.NAlbakri,B.Mansoor,H.Nassar,M.K.KhairshethThermo-mechanicalandmetallurgicalaspectsinfrictionstirprocessingofAZ31(2012)
3. FengAH, and Ma ZY, Scripta Mater 56(2007)397.17. Freeney TA, and Mishra R S, Metall Mater Trans A41(2010)73.
4. FengAH, and Ma ZY, Scripta Mater 56(2007)397.17. Freeney TA, and Mishra R S, Metall Mater Trans A41(2010)73.

5. Jayaraman M, Sivasubramanian R, and Balasubramanian V, *J Mater Sci Technol* 25 (2009)655.
6. Marek St. We, glowski Friction stir processing technology – new opportunities,weldinginternational(2014).
7. F.K. Abu-Farha, M.K. Khraisheh, *J Mater Eng Perform*, 16 (2007)192-199.
8. Friction stir processing of commercial AZ31 magnesium alloy B.M. Darras, M.K. Khraisheh *, F.K. Abu-Farha, M.A.Omar.
9. R.S. Mishraa,*, Z.Y. Mab, *Friction stir welding andprocessing*(2005).
10. “Fabricaton and optimization of FSP parameters on the properties of aluminium surface composites”,Annauniversity,Chennai,2018.
11. S. Cartigueyen, K. Mahadevan, *IOSR Journal of Mechanical and Civil Engineering*(IOSR-JMCE)
12. S.Ugendra , A.Kumar b , A. Somi Reddy a,b**Microstructure and Mechanical Properties of AZ31B Magnesium alloy by Friction stir Welding*(2014).
13. Mishra R.S Ma ZY.FSW AND Processing, *Mater.Sci.Eng R* 2005;50:1-78.
14. Ganta Venkateswarlu – M Joseph Davidson – PullaSammaiah.
15. Ganta Venkateswarlu – M Joseph Davidson – PullaSammaiah.
16. Ganta Venkateswarlu – M Joseph Davidson – PullaSammaiah.
17. A.Alavi Nia, S.H.Nourbakhsh , “Microstructure and Mechanical Properties of AZ31/SiC and AZ31/CNT Composites Produced by Friction Stir Processing”, in Elsevier Journal, 25 August2015
18. A.Alavi Nia, S.H.Nourbakhsh , “Microstructure and Mechanical Properties of AZ31/SiC and AZ31/CNT Composites Produced by Friction Stir Processing”, in Elsevier Journal, 25 August2015.
19. Yuan W, and Mishra R S, *Mater Sci Eng J* 558 (2012)716.
20. Chawla N, and Shen Y L, *Adv Eng Mater* 3 (2001)357.
21. A.Alavi Nia, S.H.Nourbakhsh , “Microstructure and Mechanical Properties of AZ31/SiC and AZ31/CNT Composites Produced by Friction Stir Processing”, in Elsevier Journal, 25 August2015.
22. F Y Lan1 , H M Chen2 , W P Guo3 , J Zhang4 and Y X Jin5 *IOP Conf. Series: Materials Science and Engineering* 230 (2017)012013.
23. P. Asadi, R.A. Mahdavinejad, S. Tutunchila. *Simulation and experimental investigation of FSP of AZ91 magnesium alloy. Materials Science and Engineering A* 528 (2011)6469-6477
24. F Y Lan1 , H M Chen2 , W P Guo3 , J Zhang4 and Y X Jin5 *IOP Conf. Series: Materials Science and Engineering* 230 (2017)012013.
25. P. Asadi, R.A. Mahdavinejad, S. Tutunchila. *Simulation and experimental investigation of FSP of AZ91 magnesium alloy. Materials Science and Engineering A* 528 (2011)6469-6477.
26. F Y Lan1 , H M Chen2 , W P Guo3 , J Zhang4 and Y X Jin5 *IOP Conf. Series: Materials Science and Engineering* 230 (2017)012013.
27. Morisada Y, Fujii H, Nagaoka T, and Fukusumi M, *Mater Sci Eng J* 433 (2006)50.
28. A. Alavi Nia1 , S. H. Nourbakhsh, *The Indian Institute of Metals – IIM*, 25 August2015.
29. Morisada Y, Fujii H, Nagaoka T, and Fukusumi M, *Mater Sci Eng J* 433 (2006)50.
30. Asadi P, Faraji G, Masoumi A, and Besharati M K, *Metall Mater Trans A* 42A (2011) 2820. 22.Sun.
31. K, Shi Q Y, Sun Y J, and Chen G Q, *Mater Sci Eng* 547 (2012)32.
32. Izadi H, and Gerlich A P, *Carbon* J 50 (2012)12.
33. Lim D K, Shibayanagi T, and Gerlich A P, *Mater Sci Eng* 507 (2009)194.
34. A. Alavi Nia1 , S. H. Nourbakhsh, *The Indian Institute of Metals - IIM*2015.
35. G.VenkateswarluInternationalJournalofAdvancementsinTechnology.
36. G.VenkateswarluInternationalJournalofAdvancementsinTechnology.
37. Callister WD (2007) *Materials science and engineering: an introduction*. Wiley,USA.
38. M. Abbasi & B. Bagheri & M. Dadaei & H. R. Omidvar & M. Rezaei Received: 8 August 2014 /Accepted: 9 November 2014 # Springer-Verlag London2014.
39. Ma ZY, Pilchak AL, Juhas MC, Williams JC (2008) *Microstructural refinement and property enhancement of cast light alloys via friction stir processing*. *Scripta Mater* 58:361–36618.
40. Tutunchilar S, Haghpanahi M, Besharati Givi MK, Asadi P, Bahemmat P (2012) *Simulation of*

material flow in friction stir processing of a cast Al- Si alloy. Mater Des 40:415–426.

- 41. Dolatkhah A, Golbabaei P, Besharati Givi M K, and Molaiekiya F, Mater Des J 37 (2012)458.
- 42. Izadi H, and Gerlich A P, Carbon J 50 (2012)12.
- 43. Zahmatkesh B, and Enayati M H, Mater Sci Eng J 527 (2010)6734.
- 44. Asadi P, Faraji G, and Besharati M K, Int J Adv Manuf Technol 51 (2010)247.
- 45. Sarkar AD (1976) Wear of metals. Elsevier,USA.
- 46. Abbasi & B. Bagheri & M. Dadaei & H. R. Omidvar & M. ,Springer-Verlag London2014.
- 47. Archard JF (1953) Contact and rubbing of flat surfaces. J Appl Phy24:981–995.
- 48. Abbasi&B.Bagheri&M.Dadaei&H.R.Omidvar&M. ,Springer-VerlagLondon2014.
- 49. Abbasi&B.Bagheri&M.Dadaei&H.R.Omidvar&M. ,Springer-VerlagLondon2